J|A|C|S
ARTICLES
Published on Web 11/22/2002

Direct Detection by Atomic Force Microscopy of Single Bond Forces Associated with the Rupture of Discrete Charge-Transfer Complexes

Hjalti Skulason and C. Daniel Frisbie*

Contribution from the Department of Chemical Engineering and Materials Science, University of Minnesota, 421 Washington Avenue SE, Minneapolis, Minnesota 55455

Received August 9, 2002

Abstract: Atomic force microscopy (AFM) was used to measure the chemical binding force of discrete electron donor−acceptor complexes formed at the interface between proximal self-assembled monolayers (SAMs). Derivatives of the well-known electron donor *N*,*N*,*N*′,*N*′-tetramethylphenylenediamine (TMPD) and the electron acceptor 7,7,8,8-tetracyanoquinodimethane (TCNQ) were immobilized on Au-coated AFM tips and substrates by formation of SAMs of *N*,*N*,*N*′-trimethyl-*N*′-(10-thiodecyl)-1,4-phenylenediamine (**I**) and bis(10-(2-((2,5-cyclohexadiene-1,4-diylidene)dimalonitrile))decyl) disulfide (**II**), respectively. Pull-off forces between modified tips and substrates were measured under $CHCl_3$ solvent. The mean pull-off forces associated with TMPD/TCNQ microcontacts were more than an order of magnitude larger than the pull-off forces for TMPD/TMPD and TCNQ/TCNQ microcontacts, consistent with the presence of specific charge-transfer interactions between proximal TMPD donors and TCNQ acceptors. Furthermore, histograms of pull-off forces for TMPD/TCNQ contacts displayed 70 ± 15 pN periodicity, assigned to the rupture of individual TMPD−TCNQ donor−acceptor (charge-transfer) complexes. Both the mean pull-off force and the 70 pN force quantum compare favorably with a contact mechanics model that incorporates the effects of discrete chemical bonds, solvent surface tensions, and random contact area variations in consecutive pull-offs. From the 70 pN force quantum, we estimate the single bond energy to be ∼4−5 kJ/mol, in reasonable agreement with thermodynamic data. These experiments establish that binding forces due to discrete chemical bonds can be detected directly in AFM pull-off measurements employing SAM modified probes and substrates. Because SAMs can be prepared with a wide range of exposed functional groups, pull-off measurements between SAM-coated tips and substrates may provide a general strategy for directly measuring binding forces associated with a variety of simple, discrete chemical bonds, e.g., single hydrogen bonds.

Introduction

Quantitative knowledge of chemical binding forces is important for a fundamental understanding of a diverse range of dynamical phenomena including molecular recognition, protein folding, interfacial adhesion, fracture, and friction.[1] In the past decade, direct force measurement methods such as optical tweezers[2] and atomic force microscopy (AFM)[3,4] have provided important experimental approaches to probing the rupture mechanics of discrete, biological ligand−receptor pairs and the dynamical stretching of individual macromolecules. However, direct force measurements of bond strengths for simple chemical interactions, e.g., hydrogen bonds,[5] generally have been much less successful than studies of macromolecular binding and stretching mechanics. Notable exceptions are the recent AFM measurements of Au−S and Si−Si single bond rupture strengths by Gaub[6] and Güntherodt,[7] respectively. Despite these recent successes, a general methodology (AFM or otherwise) has not emerged for probing directly the mechanics of *simple* chemical bonds between pairs of nonbiological molecules.

In principle, an attractive approach is to measure pull-off forces between AFM tips and substrates coated with comple-

* Address correspondence to this author. Email: frisbie@cems.umn.edu.

(1) (a) Israelachvili, J. *Intermolecular & Surface Forces*; Academic Press: New York, 1992. (b) Ulman, A. *Introduction to Ultrathin Organic Films*; Academic Press: New York, 1991. (c) Fersht, A. *Enzyme Structure and Mechanics*; W. H. Freeman: New York, 1985.
(2) (a) Meiners, J.-C.; Quake, S. R. *Phys. Rev. Lett.* **2000**, *84*, 5015. (b) Shivashankar, G. V.; Libchaber, A. *Appl. Phys. Lett.* **1997**, *71*, 3727. (c) Smith, S. B.; Cui, Y.; Bustamante, C. *Science* **1996**, *271*, 795.
(3) (a) Harada, Y.; Kuroda, M.; Ishida, A. *Langmuir* **2000**, *16*, 708. (b) Hinterdorfer, P.; Baumgartner, W.; Gruber, H. J.; Schilcher, K.; Schindler, H. *Proc. Natl. Acad. U.S.A.* **1996**, *93*, 3477. (c) Dammer, U.; Hegner, M.; Anselmetti, D.; Wagner, P.; Dreier, M.; Huber, W.; Güntherodt, H.-J. *Biophys. J.* **1996**, *70*, 2437. (d) Noy, A.; Vezenov, D. V.; Kayyem, J. F.; Meade, T. J.; Lieber, C. M. *Chem. Biol.* **1997**, *4*, 519−27. (e) Moy, V. T.; Florin, E.-L.; Gaub, H. E. *Science* **1994**, *266*, 257. (f) Florin, E.-L.; Moy, V. T.; Gaub, H. E. *Science* **1994**, *264*, 415. (g) Lee, G. U.; Chrisey, L. A.; Colton, R. J. *Science* **1994**, *266*, 771.
(4) (a) Oberhauser, A. F.; Marszalek, P. E.; Erickson, H. P.; Fernandez, J. M. *Nature* **1998**, *393*, 181. (b) Marszalek, P. E.; Oberhauser, A. F.; Pang, Y.-P.; Fernandez, J. M. *Nature* **1998**, *396*, 661. (c) Rief, M.; Oesterhelt, F.; Heymann, B.; Gaub, H. E. *Science* **1997**, *275*, 1295. (d) Rief, M.; Gautel, M.; Oesterhelt, F.; Fernandez, J. M.; Gaub, H. E. *Science* **1997**, *276*, 1109. (e) Misui, K.; Hara, M.; Ikai, A. *FEBS Lett.* **1996**, *385*, 29.
(5) Hoh, J. H.; Cleveland, J. P.; Prater, C. B.; Revel, J.-P.; Hansma, P. K. *J. Am. Chem. Soc.* **1992**, *114*, 4917.
(6) Grandbois, M.; Beyer, M. Rief, M.; Clausen-Schaumann, H.; Gaub, H. E. *Science* **1999**, *283*, 1727.
(7) Lantz, M. A.; Hug, H. J.; Hoffmann, R.; van Schendel, P. J. A.; Kappenberger, P.; Martin, S.; Baratoff, A.; Güntherodt, H.-J. *Science* **2001**, *291*, 2580.

Scheme 1. Specific Chemical Bonds Are Formed and Broken Between Complementary Self-assembled Monolayers (SAMs) When the AFM Probe Is Repeatedly Brought into Contact with the Substrate and Then Pulled Off

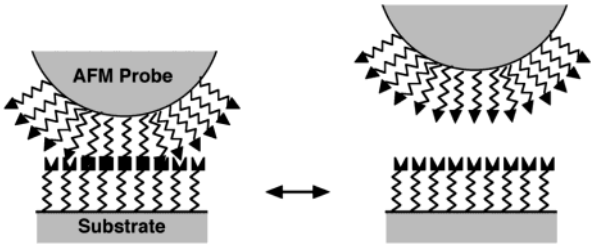

mentary self-assembled monolayers (SAMs) capable of specific chemical binding, Scheme 1.[8] In a pull-off experiment, exposed functional groups on the two SAM surfaces bind upon tip−substrate contact; the binding is quantified by measuring the pull-off force required to rupture the contact. Because of the sharpness of the tip, the contact area is on the order of a few nm^2, so that pull-off involves breaking a small integer number of bonds. Fluctuations in the number of discrete bonds formed and broken in consecutive pull-off measurements (in which the adhesive contact between the tip and substrate is made and broken multiple times) give rise to a distribution of forces. This distribution, plotted as a histogram of pull-off forces, can be analyzed to determine the "force quantum" associated with the rupture of single chemical bonds.

The histogram approach is well recognized and has yielded single bond forces in specific cases involving biological ligand−receptor interactions[3e,f] or SAMs containing complementary DNA strands.[3d,g] However, direct detection of single bonds has not been reported for experiments involving tips and substrates modified with functionalized SAMs capable of simple, specific interactions, such as hydrogen bonding or charge-transfer complexing. This is particularly surprising given that SAM modified tips and substrates appear to be ideal systems for pull-off experiments because the exposed terminal functional groups can be changed easily and systematically. It is also well-known that the *average* pull off forces for SAM-modified tips depend on the surface energies of the SAMs,[8] meaning that the exposed functional groups do affect measured rupture forces.

Using a modified Johnson−Kendall−Roberts (JKR) contact mechanics model, we have recently analyzed the problem of detecting single bond forces in AFM pull-off measurements and have concluded that there are stringent requirements on the tip−substrate interfacial energy, tip radius, and the bond formation probability.[9] The JKR theory[10] relates the pull-off force, $F_{\mathrm{Pull-Off}}$ (N), to the thermodynamic work of adhesion, W_{Ad} (J/m^2), according to eq 1

$$F_{\mathrm{Pull-Off}} = \frac{3\pi R W_{\mathrm{Ad}}}{2} \tag{1}$$

where R is the radius of curvature of the tip. To avoid the effects of capillary condensation around the microcontact, AFM pull-off measurements are typically carried out under solvent. In the presence of solvent, W_{Ad} is defined as

$$\begin{aligned} W_{\mathrm{Ad}} &= \gamma_{\mathrm{Substrate-Solvent}} + \gamma_{\mathrm{Probe-Solvent}} - \gamma_{\mathrm{Probe-Substrate}} \\ &= \gamma_{\mathrm{Solvent}} - \gamma_{\mathrm{Probe-Substrate}} \end{aligned} \tag{2}$$

where $\gamma_{\mathrm{Substrate-Solvent}}$ (J/m^2) and $\gamma_{\mathrm{Probe-Solvent}}$ (J/m^2) are the interfacial free energies of the solvent with the substrate and the probe and $\gamma_{\mathrm{Probe-Substrate}}$ (J/m^2) is the interfacial free energy between the probe and the substrate. For convenience, we have defined $\gamma_{\mathrm{Solvent}}$ as the sum of the two interfacial energies involving the solvent. A key point is that in order for the pull-off measurements to be sensitive to the formation of discrete bonds in the microcontact, W_{Ad} must be dominated by $\gamma_{\mathrm{Probe-Substrate}}$, which represents the bonding interactions, and not by $\gamma_{\mathrm{Solvent}}$. Referring to eq 2, this leads to the dual requirements that $\gamma_{\mathrm{Probe-Substrate}} < 0$ (it must be negative) and $|\gamma_{\mathrm{Probe-Substrate}}| > \gamma_{\mathrm{Solvent}}$, to achieve a large positive contribution of specific tip−substrate binding to W_{Ad}.[11] Many previous AFM pull-off experiments have been carried out under conditions where these requirements were not met,[8a,c−n] and so discrete forces in pull-off force histograms were not observed. For single bond detection, it is also important that the tip−substrate contact area be small, of order 10 nm^2 or less, so that pull-off involves breaking a small number of bonds; this means that the tip must be sharp. In addition, the bond formation probability must be high, typically greater than 90%, such that the pull-off forces are dominated by specific, not nonspecific, interactions. This means, for example, that for a typical contact area of 5 nm^2 between SAM-modified tips and substrates, 9 of 10 possible bonds form *on average*.

Because of these requirements, we have concentrated on identifying complementary SAM systems that are capable of strong, specific interactions and that are compatible with solvents exhibiting low interfacial tensions (small $\gamma_{\mathrm{Solvent}}$). In this paper, we report the successful detection of single bond forces in AFM pull-off experiments employing SAM-modified tips and substrates bearing electron donors and acceptors. We used reagents **I** and **II** to attach derivatives of the electron donor *N*,*N*,*N*′,*N*′-tetramethyl-*p*-phenylenediamine (TMPD) and the electron acceptor 7,7,8,8-tetracyanoquinodimethane (TCNQ), respectively, to Au-coated tips and substrates through alkane thiol monolayer formation. TMPD and TCNQ are ubiquitous in charge-transfer chemistry due to their exceptionally strong electron donating

(8) (a) Smith, D. A.; Wallwork, M. L.; Zhang, J.; Kirkham, J.; Robinson, C.; Marsh, A.; Wong, M. *J. Phys. Chem. B* **2000**, *104*, 8862. (b) Skulason, H.; Frisbie, C. D. *J. Am. Chem. Soc.* **2000**, *122*, 9750. (c) Lo, Y.-S.; Huefner, N. D.; Chan, W. S.; Stevens, F.; Harris, J. M.; Beebe, T. P. *Langmuir* **1999**, *15*, 1373. (d) Ito, T.; Citterio, D.; Bühlmann, P.; Umezawa, Y. *Langmuir* **1999**, *15*, 2788. (e) Clear, S. C.; Nealey, P. F. *J. Colloid Intface Sci.* **1999**, *213*, 238. (f) McKendry, R. A.; Theoclitou, M.-E.; Rayment, T.; Abell, C. *Nature* **1998**, *391*, 566. (g) van der Vegte, E. W.; Hadziioannou, G. *Langmuir* **1997**, *13*, 4357. (h) Noy, A.; Vezenov, D. V.; Lieber, C. M. *Annu. Rev. Mater. Sci.* **1997**, *27*, 381−427. (i) Sinniah, S. K.; Steel, A. B.; Miller, C. J.; Reutt-Robey, J. E. *J. Am. Chem. Soc.* **1996**, *118*, 8925. (j) Green, J.-B. D.; McDermott, M. T.; Porter, M. D. *J. Phys. Chem.* **1996**, *100*, 13342. (k) Noy, A.; Frisbie, C. D.; Rozsnyai, L. F.; Wrighton, M. S.; Lieber, C. M. *J. Am. Chem. Soc.* **1995**, *117*, 7943. (l) Han T.; Williams, J. M.; Beebe, T. P. *Anal. Chim. Acta* **1995**, *307*, 365. (m) Thomas, R. C.; Houston, J. E.; Crooks, R. M.; Kim, T.; Michalske, T. A. *J. Am. Chem. Soc.* **1995**, *117*, 3830. (n) Nakagawa, T.; Ogawa, K.; Kurumizawa, T. *J. Vac. Sci. Technol. B* **1994**, *12*, 2215.
(9) Skulason, H.; Frisbie, C. D. *Anal. Chem.* **2002**, *74*, 3096.
(10) Johnson, K. L.; Kendall, K.; Roberts, A. D. *Proc. R. Soc. London A.* **1971**, *324*, 301.

(11) Negative *interfacial* energies are possible and reflect bonding interactions at the interface. The work of adhesion between two media 1 and 2 in a vacuum is given by $W_{\mathrm{Ad}} = \gamma_1 + \gamma_2 - \gamma_{12}$, where γ_1 and γ_2 are surface energies and γ_{12} is an interfacial energy. This equation is essentially the definition of interfacial energy (as distinct from *surface* energies γ_1 and γ_2, which are always positive). It is clear that if W_{Ad} is large, γ_{12} can be negative. Equation 2 in the text defines work of adhesion completely in terms of interfacial energies because the pull-off experiment is carried out under solvent. Any of the interfacial energy terms in eq 2 can be positive or negative in principle.

and accepting properties.[12] When solutions of TMPD and TCNQ are mixed, the following equilibria are established

$$\text{TMPD} + \text{TCNQ} \rightleftharpoons [\text{TMPD-TCNQ}] \rightleftharpoons \text{TMPD}^{+\bullet} + \text{TCNQ}^{-\bullet} \quad (3)$$

where [TMPD−TCNQ] represents a CT complex, Scheme 2a. The formation constant K_{eq} for [TMPD−TCNQ] in $CHCl_3$ at 293 K is 360 M^{-1}.[13] Thus, the free energy of formation, ΔG_f°, is −14 kJ/mol (−0.14 eV), comparable to that for H-bonds.

We have already shown in previous work that SAMs of **I** and **II** are redox-active and capable of forming inter-monolayer charge-transfer (CT) complexes.[14] For completeness, we report in this paper the equilibrium constant for [**Ia**−**II**] complexes in $CHCl_3$ solution obtained using UV−vis spectroscopy. We used **Ia** instead of **I** for the solution studies because we have found that **II** will react with free −SH groups.[15]

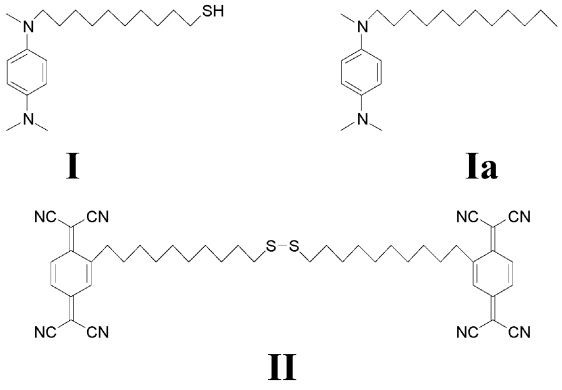

We measured pull-off forces under $CHCl_3$ between tips and substrates modified with SAMs of **I** or **II**, Scheme 2b. The average pull-off forces required to rupture **I**−**II** microcontacts were up to 20 times larger than pull-off forces obtained in control experiments where complex formation was absent, indicating that specific interactions between **I** and **II** were responsible for the large adhesion. Furthermore, measurements of hundreds of consecutive probe−substrate pull-offs revealed a 70 ± 15 pN force quantum, which we have assigned to the mechanical rupture of *individual* TMPD−TCNQ CT complexes.

To our knowledge, these are the first reported measurements of single bond forces associated with discrete, nonbiological interactions between proximal SAMs. Because of the structural flexibility of SAMs, our demonstrated ability to detect single bond forces between proximal SAMs in microcontact pull-off experiments may point to a general approach for measuring rupture forces associated with a wide variety of simple chemical bonds.

Experimental Section

Materials. All solvents used were of spectroscopic quality, and $CHCl_3$ was distilled from P_2O_5. Absolute ethanol was obtained from Aaper Alcohol and Chemical Co. (Shelbyville, KY). Gold (99.999%) was obtained from W. E. Mowrey Co. (St. Paul, MN) and chromium-coated W rods from R. D. Mathis (Long Beach, CA). Silicon wafers were purchased from WaferNet (San Jose, CA), and standard Si_3N_4 triangular cantilevers were obtained from Digital Instruments (Santa Barbara, CA). Water (18MΩ) was filtered using a Barnstead system. **I** and **II** were synthesized as described previously,[14] and **Ia** was similarly synthesized using dodecyliodide as a starting material.

Scheme 2. (A) Formation of a CT Complex Between TMPD and TCNQ. (B) Schematic Representation of CT Complex Formation Between a SAM of **I** on an Au Coated AFM Probe and a SAM of **II** on an Au Substrate

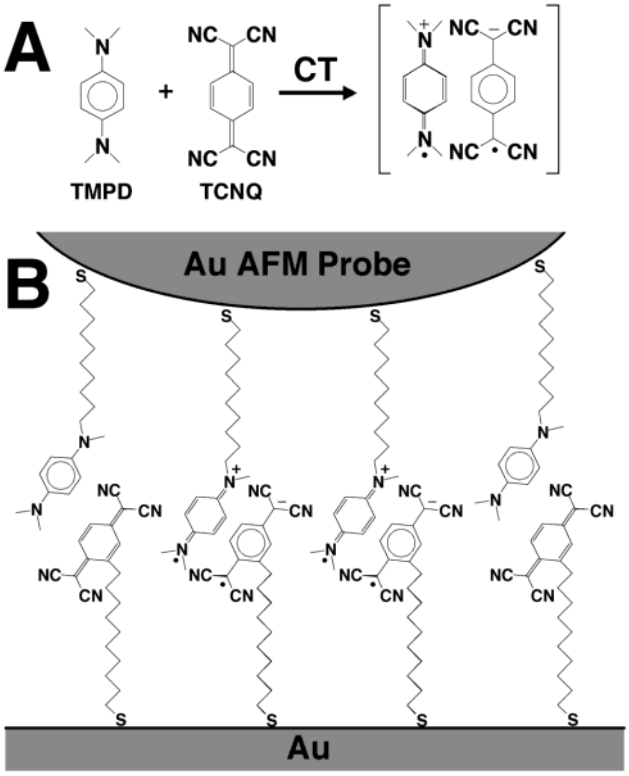

Monolayer Preparation. Silicon wafers, cut into 10 × 10 mm pieces, were cleaned in boiling 5:1:1 $H_2O/H_2O_2/NH_4OH$, rinsed with distilled water and absolute ethanol, and dried with flowing N_2. Following thermal evaporation of a 5 nm Cr adhesion layer and 100 nm of Au, the slides were immersed in the respective reagent solution (**I** in C_6H_6 and **II** in CH_2Cl_2) for 1 h followed by extensive rinsing with the neat solvent and drying with flowing N_2. Chemical derivatization of cantilevers was carried out in a similar way except they were rinsed with CH_2Cl_2 prior to evaporation of 5 nm Cr and 40 nm of Au.

Infared Spectroscopy. Infrared spectra were recorded using a Nicolet MAGNA 550 FT-IR spectrometer. Solution spectra were recorded using NaCl windows separated by a Teflon spacer. Care was taken not to let the solution come in contact with any metal surfaces, which causes reduction of the TCNQ group in **II**.

UV−Visible Spectroscopy. Absorption spectroscopy in the ultraviolet−visible range was recorded on a Hewlett-Packard 8452A diode array spectrophotometer using standard quartz cuvettes. Due to overlap between absorption peaks, the absorption spectrum was fitted with a series of Gaussian peaks and the intensity of the fitted charge-transfer absorption peak at 538 nm was used.

Pull-Off Force Measurements. Pull-off forces were measured with a PicoSPM microscope from Molecular Imaging Corporation (Phoenix, AZ) and a Nanoscope III controller from Digital Instruments (Santa Barbara, CA). Au/Cr coated V-shape Si_3N_4 cantilevers with leg length of 200 μm and leg width of 20 μm were used. The force constant of each lever was determined by the Cleveland method.[16] Resonance frequencies of coated cantilevers varied from 15.7 to 16.5 kHz, with corresponding variation of the force constant between 0.059 and 0.066

(12) (a) Ward, M. D. In *Electroanalytical Chemistry*; Marcel Dekker Inc.: New York, 1991; Vol. 16, p 181. (b) Wheland, R. C.; Gillson, J. L. *J. Am. Chem. Soc.* **1976**, *98*, 3916. (c) Mulliken, R. S.; Person, W. B. *Molecular Complexes*; Wiley−Interscience: New York, 1969.
(13) Yamagishi, A.; Masui, T.; Watanabe, F. *J. Colloid Interface Sci.* **1979**, *72*, 154.
(14) Skulason, H.; Frisbie, C. D. *Langmuir* **1998**, *14*, 5834.
(15) Skulason, H.; Frisbie, C. D., unpublished results.

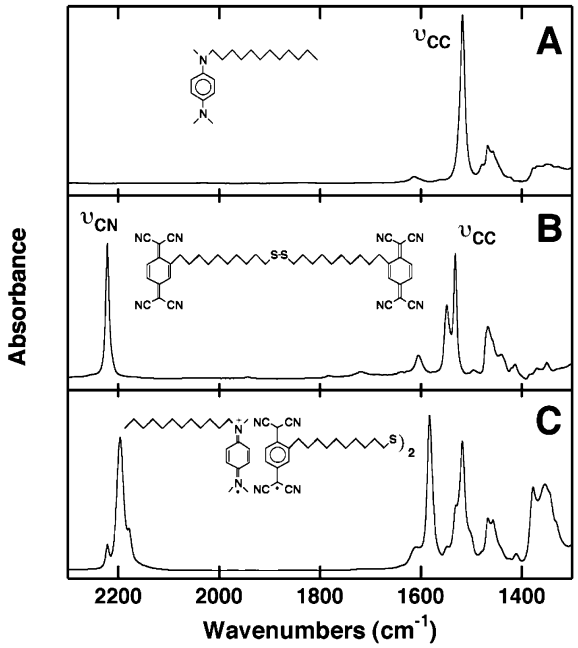

Figure 1. (A) Solution IR spectrum of **Ia** in $CHCl_3$. The principal peak at 1518 cm^{-1} corresponds to a C═C ring mode stretch. (B) Solution IR spectrum of **II** in $CHCl_3$. Principal peaks correspond to C≡N (2222 cm^{-1}) and C═C (1549 and 1532 cm^{-1}) stretches. (C) Solution IR spectrum of **Ia** and **II** in $CHCl_3$. New stretches at 2197, 2179, and 1583 cm^{-1} are characteristic of reduced TCNQ while the peak at 1377 cm^{-1} stems from oxidized TMPD.

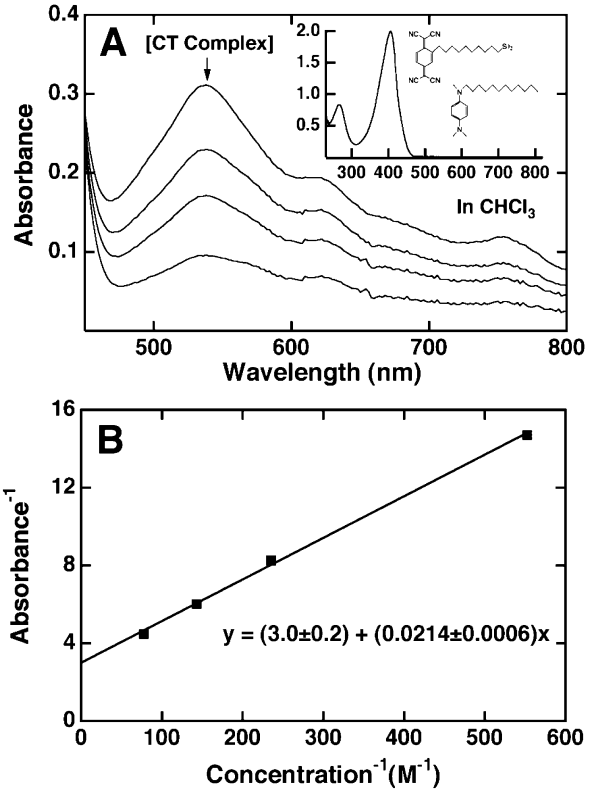

Figure 2. (A) Electronic absorption spectra of $CHCl_3$ solutions of **Ia** (1.81, 4.25, 7.00, and 12.9 mM) and **II** (0.113 mM), showing the region of the CT absorption peak at 538 nm and the entire range of the measured spectrum (inset). (B) Plot of the inverse absorption of the CT peak at 538 nm vs the inverse concentration of **Ia**. Following the method of Benesi and Hildebrand,[22] the ratio of the intercept and the slope of the linear fit to the data yields the equilibrium constant for the CT complex formation, $K_{eq} = 140 \pm 10$ M^{-1}.

N/m. Force measurements were typically carried out with a Z position sweep of 75 nm at a rate of 75 nm/s. Blocking of a SAM of **II** was carried out by adding 3 drops of a 0.1 M $CHCl_3$ solution of **Ia**. Force curves were analyzed using routines written in Igor Pro (Wavemetrics, Lake Oswego, OR). For each force curve, drift and nonlinearity of the photodetector were corrected by giving the contact region of the retraction curve a slope of −1. The smoothly varying background of the autocorrelation function was subtracted by application of a 30th order binomial filter.[17]

Results

Solution Spectroscopy. Transmission infrared and UV−visible spectroscopies were used to verify the formation of a charge-transfer complex between **Ia** and **II** in $CHCl_3$ solution. Figure 1a shows the IR spectrum of **Ia** in $CHCl_3$. The principal peaks at 1518, 1468, and 1457 cm^{-1} are due to a C═C ring breathing mode in the phenylene unit[18] and CH_2 scissoring and CH_3 bending modes, respectively. Figure 1B shows the IR spectrum of **II** in $CHCl_3$. A C≡N stretch is positioned at 2222 cm^{-1}, two C═C ring modes at 1549 and 1532 cm^{-1}, and a CH_2 scissor at 1468 cm^{-1}.[19] The IR spectrum of a $CHCl_3$ solution containing both **Ia** and **II** is shown in Figure 1C. New peaks that can be assigned to the $TCNQ^{-\bullet}$ group appear at 2197 (C≡N), 2179 (C≡N), 1583 (C═C), and 1354 cm^{-1} (C−H bend) and to the $TMPD^{+\bullet}$ group at 1377 cm^{-1} (C−N).[20] Other peaks are unchanged from Figure 1A (1518 and 1467 cm^{-1}) and Figure 1B (2222, 1530 (shoulder), and 1467 cm^{-1}). These results demonstrate that upon mixing of **Ia** and **II** in $CHCl_3$ the TMPD group in **Ia** is oxidized to form a radical cation and the TCNQ group in **II** is reduced to form a radical anion.

To verify the formation of a charge-transfer complex, and to determine its equilibrium constant, absorbances in the UV−vis spectrum of a 0.1 mM $CHCl_3$ solution of **Ia** and **II** were recorded, Figure 2. The inset in Figure 2A shows the UV−vis spectrum from 150 to 800 nm. The spectrum appears to be the sum of the individual UV−vis spectra of **Ia** and **II**. **Ia** has two absorbance peaks at 268 and 330 nm which overlap with the absorbance at 406 nm from **II**. However, additional weak absorption peaks appear at 538, 568, 622, and 756 nm, which are shown in Figure 2A. Comparison to spectra of $CHCl_3$ solutions of the radical cation of **Ia** and the radical anion of **II**, respectively, reveals that the peaks at 568 and 622 nm can be assigned to $\mathbf{Ia}^{+\bullet}$ and the peak at 756 nm to $\mathbf{II}^{-\bullet}$. The peak at 538 nm is ascribed to an absorption of the charge-transfer complex of **Ia** and **II** ($CHCl_3$ solutions of TMPD and TCNQ show a CT band at 530 nm).[21] The appearance of a CT absorption peak (538 nm) and peaks corresponding to the separated molecular ions suggests an equilibrium mixture of neutral, complexed, and ionic species as shown in eq 3. Separated molecular ions are not observed for TMPD and TCNQ

(16) Cleveland, J. P.; Manne, S.; Bocek, D.; Hansma, P. K. *Rev. Sci. Instrum.* **1993**, *64*, 403.
(17) Marchard, P.; Marmet, L. *Rev. Sci. Instrum.* **1983**, *54*, 1034.
(18) Kubinyi, M.; Varsanyi, G.; Grofcsik, A. *Spectrochim. Acta* **1980**, *36A*, 265.
(19) Takenaka, T. *Spectrochim. Acta* **1971**, *27A*, 1735.
(20) (a) Girlando, A.; Painelli, A.; Pecile, C. *Mol. Cryst. Liq. Cryst.* **1984**, *112*, 325. (b) Bozio, R.; Zanon, I.; Girlando, A.; Pecile, C. *J. Chem. Soc., Faraday Trans. 2* **1978**, *74*, 235. (c) Bozio, R.; Girlando, A.; Pecile, C. *J. Chem. Soc., Faraday Trans. 2* **1975**, *71*, 1237. (d) Kuroda, H.; Hiroma, S.; Akamatu, H. *Bull. Chem. Soc. Jpn.* **1968**, *41*, 2855.
(21) Yamagishi, A.; Masui, T.; Watanabe, F. *J. Colloid Interface Sci.* **1979**, *72*, 154.

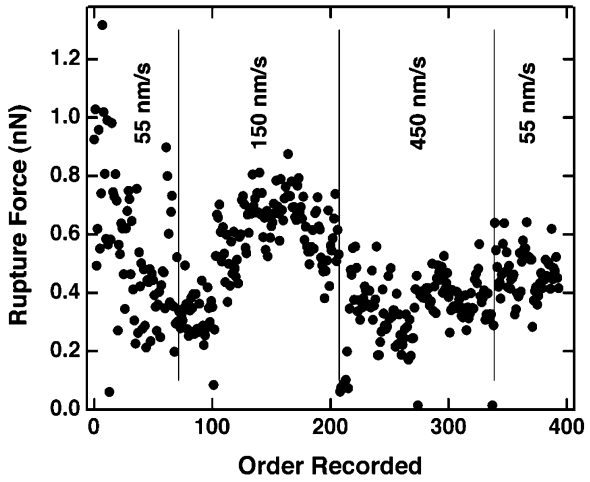

Figure 3. Recorded force required to rupture a **I**/**II** contact in $CHCl_3$ during the span of an experiment. The vertical lines show the division between different scan rates at which the rupture forces were recorded.

in $CHCl_3$. The difference can likely be attributed to the higher solubility of $\mathbf{Ia}^{+\bullet}$ and $\mathbf{II}^{-\bullet}$ in $CHCl_3$.

Following the method of Benesi and Hildebrand,[22] the absorbance of the CT complex, A_{538}^{CT}, can be related to the concentration of **Ia** by

$$\frac{1}{A_{538}^{\ CT}} = \frac{1}{\epsilon_{538} b C_{II}}\left(1 + \frac{1}{K_{eq} C_{Ia}}\right) \tag{4}$$

where ϵ_{538} is the molar absorptivity of the complex, b is the path length, C_{Ia} and C_{II} are the concentrations of **Ia** and **II**, respectively, with $C_{Ia} \gg C_{II}$, and K_{eq} is the equilibrium constant.

$$K_{eq} = \frac{[\mathbf{Ia} - \mathbf{II}]}{[\mathbf{Ia}][\mathbf{II}]} \tag{5}$$

Figure 2A shows the absorption spectra of four solutions, all 0.11 mM in **II** and 1.81−12.0 mM in **Ia**. The inverse absorbance of the CT complex determined from these spectra is plotted versus the inverse concentration of **Ia** in Figure 2B. A linear fit of the data in Figure 2B (solid trace) yields a slope of 21.4 ± 0.6 mM and a y-axis intercept of 3.0 ± 0.2 which gives $K_{eq} = (1.4 \pm 0.1) \times 10^2\ M^{-1}$ and $\epsilon_{538} = (3.0 \pm 0.2) \times 10^3\ cm^{-1}\ M^{-1}$. While the IR solution spectra demonstrate that electron transfer from **Ia** to **II** takes place, the UV−vis spectra show that this CT is accompanied by complex formation.

Pull-Off Force Measurements. Figure 3 shows consecutively measured pull-off forces at different scan rates between a SAM of **I** on an Au substrate and an Au probe derivatized with **II**. No correlation is observed between the measured pull-off force and the scan rate although the average force does change slowly during the time span of the experiment. The gradual change in the pull-off force does not seem to be caused by degradation of the monolayers since that would lead to monotonically declining forces. Instead, the variation in the average force points toward variation in the contact area due to the inherent roughness of the polycrystalline gold substrate and the slow drift (∼0.3 nm/s) of the AFM probe across the surface (see Discussion).

Figures 4A and 4B show histograms of pull-off forces for **I**−**II** microcontacts in $CHCl_3$, before and after addition of **Ia** as a blocking agent. The data set in Figure 4A represents 400 consecutive pull-offs for the same tip coated with a SAM of **I**

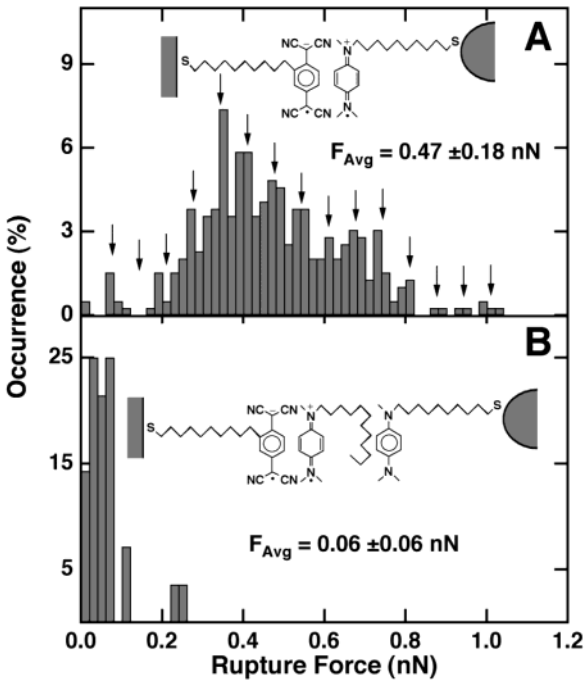

Figure 4. (A) Histogram of pull-off forces for a SAM of **I** on an Au coated AFM probe contacting a SAM of **II** on an Au substrate in $CHCl_3$. Arrows point to peaks with a periodicity of 70 pN, associated with the rupture of individual bonds. (B) Histogram of pull-off forces recorded after the addition of **Ia** to the $CHCl_3$ which forms a CT complex to **II** on the substrate.

contacting a substrate with a SAM of **II**; the mean pull-off force is 0.47 ± 0.18 nN. Addition of **Ia** to the $CHCl_3$ solution caused the mean pull-off force to drop by a factor of 8 to 0.06 ± 0.06 nN, Figure 4B. The observation of a lower mean force is consistent with the expectation that **Ia** will bind to SAMs of **II** and thus block specific interactions between the tip and substrate. This blocking experiment serves as an in situ control to verify that the adhesion force observed in Figure 4A arises from specific interactions between the probe tip and substrate.

Periodicity is also apparent in the Figure 4A histogram for **I**−**II** microcontacts, as highlighted by the evenly spaced arrows. This periodicity is emphasized in the autocorrelation of the histogram in Figure 5A, which shows a sinusoidal oscillation with a period of 70 pN. The 70 pN period is readily apparent in the Fourier transform of the autocorrelation function, Figure 5B, which shows a single peak.

Periodicity was observed in pull-off force histograms independent of whether **I** was grafted to the tip and **II** was grafted to the substrate (as in the Figure 4 data) or vice versa. Figure 6 shows a histogram of pull-off forces obtained for microcontacts with a SAM of **II** on the tip and **I** on the substrate. In this case the periodicity is 60 pN, as emphasized by the evenly spaced arrows. The 10 pN difference in the force quanta detected in Figures 4 and 6 reflects the precision of our measurements. For five different trials in which force quanta were detected, we obtained an average force quantum of 70 ± 15 pN.

In a second set of control experiments designed to estimate the importance of nonspecific adhesion to our measurements, we measured pull-off forces for **I**−**I** and **II**−**II** microcontacts in $CHCl_3$. Histograms of pull-off forces with either a SAM of **I** or a SAM of **II** on *both* probe and substrate are shown in Figures 7A and 7B, respectively. Adhesion between symmetric **I**−**I** or **II**−**II** contacts ($F_{Pull-Off}^{avg} = 0.02 \pm 0.03$ nN for **I**, Figure

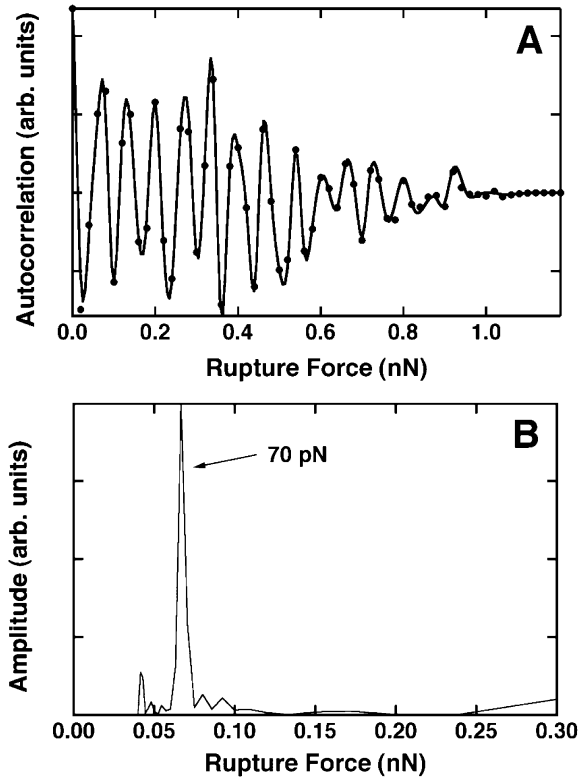

Figure 5. (A) Autocorrelation of the histogram of pull-off forces shown in Figure 4A. Oscillations have a periodicity of 70 pN which is emphasized by a single peak in the Fourier transform (B) of the autocorrelation function.

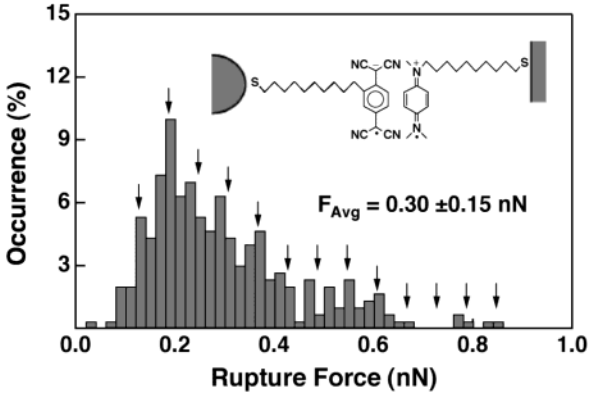

Figure 6. Histogram of pull-off forces for a SAM of **II** on an Au coated AFM probe contacting a SAM of **I** on an Au substrate in $CHCl_3$. Arrows point to peaks with periodicity of 60 pN.

7A, and $F^{avg}_{Pull-Off} = 0.02 \pm 0.04$ nN for **II**, Figure 7B), where no CT binding is expected, is more than an order of magnitude less than between asymmetric (**I**−**II**) contacts.

Discussion

Formation of a Charge-Transfer Complex between Ia and II. In previous work,[14] we have shown that SAMs of **I** and **II** on Au are redox-active and form charge-transfer complexes with TCNQ and TMPD, respectively; in that earlier study, surface-bound CT complexes were formed by immersing SAMs of **I** or **II** in C_6H_6 solutions of the complementary acceptor or donor. For the present work, we chose to measure pull-off forces for **I**−**II** microcontacts under $CHCl_3$. The choice of $CHCl_3$ was motivated by the fact that we observed smaller nonspecific adhesion (i.e., small $\gamma_{Solvent}$) in this solvent than in others we

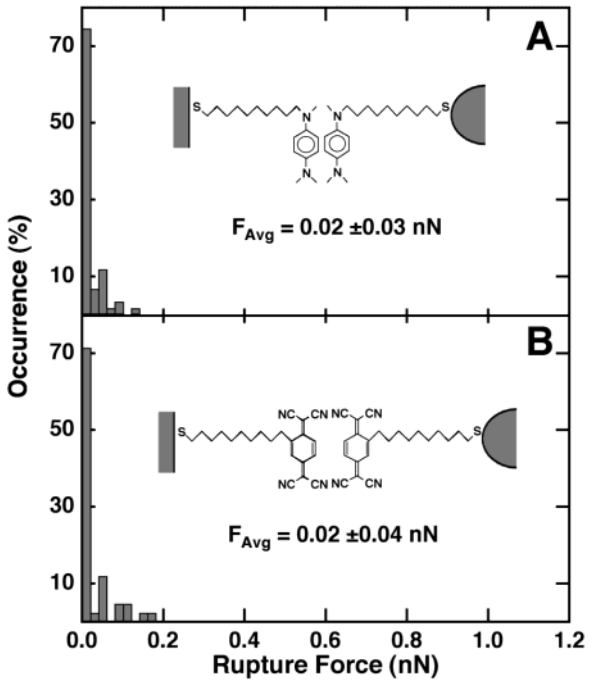

Figure 7. Histograms of pull-off forces for **I**−**I** and **II**−**II** contacts in $CHCl_3$. (A) An Au probe coated with **I** contacting an Au substrate coated with **I**. (B) An Au probe coated with **II** contacting an Au substrate also coated with **II**.

tried such as benzene, toluene, and acetonitrile. As explained in the Introduction, we used **Ia** instead of **I** for the solution studies because **II** reacts with free −SH groups. The presence of a CT absorption band at 538 nm in Figure 2 is definitive evidence that a CT complex forms between **Ia** and **II**. Transfer of charge from **Ia** to **II** is also corroborated by the solution IR data, Figure 1C, which shows stretches characteristic of the $TCNQ^{-\bullet}$ and $TMPD^{+\bullet}$ groups in the complex. The weak absorptions due to separated molecular ions in the UV−vis spectrum (568, 622, and 756 nm) confirm that **Ia** and **II** predominately form a CT complex and to a much lesser extent, separated ions.

We used the 538 nm CT band to determine the equilibrium constant ($K_{eq} = 140$ M^{-1}) for complex formation in $CHCl_3$ solutions of **Ia** and **II** at room temperature. The value is somewhat smaller than K_{eq} for [TMPD−TCNQ] complex formation in the same solvent (360 M^{-1}).[21] From the K_{eq} values, we compute $\Delta G^{\circ}_{Ia-II} = -12$ kJ/mol (0.12 eV) and $\Delta G^{\circ}_{TMPD-TCNQ} = -14$ kJ/mol (0.14 eV).[23]

The presence of alkyl chains coupled to the TMPD and TCNQ groups in **Ia** and **II** can reduce the free energy change

(22) Benesi, H. A.; Hildebrand, J. H. *J. Am. Chem. Soc.* **1949**, *71*, 2703.
(23) It interesting to compare the free energy for complex formation to the free energy, $\Delta G_{e-Transfer}$, of electron transfer from the donor to the acceptor to form molecular ions, which can be obtained from solution redox values. Using $\Delta G_{e-Transfer} = -nF\Delta E$, where n is the number of electrons transferred per molecule ($n = 1$), F is the Faraday constant, and ΔE is the difference in the one electron redox potential for the donor and the acceptor, we get $\Delta G_{e-Transfer} = 0$ kJ/mol for electron transfer between **I** and **II** and $\Delta G_{e-Transfer} = +3.9$ kJ/mol for TMPD and TCNQ. The process of electron transfer from **I** to **II** in $CHCl_3$ is more favorable than between TMPD and TCNQ due to the inductive effect of the alkyl chain in **I**, resulting in better donor properties. This is reflected by the slightly lower energy of the CT excitation of the [**I**−**II**] complex in $CHCl_3$ at 538 nm vs 530 nm for [TMPD−TCNQ]. Excitation energies of CT complexes have been shown to decrease with decreased ionization potential of the electron donor. However, **I** and **II** are less effective in forming a CT complex ($\Delta G_{Complex} = -12$ kJ/mol vs −14 kJ/mol for [TCNQ−TMPD]). This clearly shows that factors other than the redox properties of the participating molecules affect complex formation.

associated with complex formation in several ways. The most obvious effect is steric hindrance. If the TMPD and TCNQ groups in the solvated complex of **Ia** and **II** are oriented face-to-face, similar to the orientation of TMPD and TCNQ in the solid state, then the alkyl chains may prevent these groups from reaching their equilibrium separation (which is 3.3 Å in the solid state[24]). The alkyl chains may also affect the symmetry of the molecular orbitals participating in the formation of the CT complex, thereby influencing complex stabilization. Nevertheless, the stabilization energy of −12 kJ/mol means that **Ia** and **II** bind with energies comparable to H-bonds.[25] It is therefore reasonable to expect that when Au probes and substrates coated with **I** and **II** are brought into contact, CT complex formation will occur at the interface.

We can use K_{eq} to estimate the degree of complexation in a microcontact between SAMs of **I** and **II**. A value of $K_{eq} = 140$ M^{-1} means that for 1 M concentrations of both **Ia** and **II**, ~92% of the molecules are complexed. If the concentration is lowered to 0.1 M the fraction complexed drops to ~8%. If we assume that the donor and acceptor functional groups tethered to the tip and substrate have access to a free volume of 0.5 nm^3, then we can estimate the volumetric concentration of these surface-confined groups to be ~3 M. Thus, based on the solution equilibrium constant, the extent of the CT reaction within the probe−substrate contact area is expected to be very high, greater than ~95%.

Rupture of Individual Charge-Transfer Complexes. Comparison of the histograms in Figures 4, 6, and 7 reveals that the average pull-off force is up to 20 times larger for **I**−**II** microcontacts where CT complex formation can take place than for **I**−**I** and **II**−**II** microcontacts where CT complex formation is not possible. We conclude that the pull-off forces measured between SAMs of **I** and **II** are due to *specific charge-transfer interactions* between the TMPD and TCNQ groups on the probe and the substrate. This conclusion is supported by the blocking experiments in which adding **Ia** to the $CHCl_3$ solvent caused the pull-off force for **I**−**II** microcontacts to drop by a factor of 8 (Figure 4B). We also note that the small magnitude of the forces for **I**−**I** and **II**−**II** contacts (Figure 7) demonstrates the absence of significant solvent exclusion forces in our measurements,[8i] reflecting the low interfacial energy ($\gamma_{Solvent}$) between the SAMs and the $CHCl_3$ solvent.

The key result is the 70 and 60 pN periodicity in the histograms in Figures 4A and 6, respectively. We have ascribed the large adhesion between SAMs of **I** and **II** to specific interactions between the TMPD and TCNQ groups inside the probe−substrate contact area. Thus, we assign the force quantum in Figures 4 and 6 to the rupture of *individual* TMPD−TCNQ CT complexes. This force quantum (70 ± 15 pN) was observed for several different AFM probes functionalized with SAMs of either **I** or **II** in contact with the complementary SAM.[26] Inspection of Figure 4A shows the mean pull-off force corresponds to breaking of seven discrete bonds. The mean in Figure 6 corresponds to breaking of four−five bonds.

Comparison between Single Bond Rupture Forces and Bond Energies. It is important to compare the single bond force we measure with the bond energy for a single CT complex. If we assume an approximate bond rupture length of 1 Å, then a 70 ± 15 pN force quantum corresponds to a bond energy of −4 to −5 kJ/mol (−40 to −50 meV). That estimate appears to be of the right order of magnitude because the free energy of formation for the complex is −12 kJ/mol (−0.12 eV).

Scheme 3. Three Possible Rupture Paths for the TMPD-TCNQ CT Complex: (A) Separation Perpendicular to the Molecular Planes, (B) Sliding Perpendicular to the Long Molecular Axis, and (C) Sliding Parallel to the Long Molecular Axis

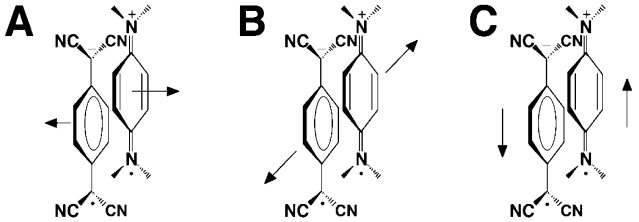

Other workers have pointed out that the relevant energy for direct force measurements is the enthalpy, $\Delta H°$, not $\Delta G°$. Calculating $\Delta H°$ from $\Delta G°$ naturally requires an estimate for the entropy of complexation, $\Delta S°$. We have not found $\Delta S°$ values for [TMPD−TCNQ], but $\Delta S°$ for other TCNQ-based CT complexes, such as [phenoxathiin−TCNQ] and [dibenzo-1,4-dioxane−TCNQ], are about 30 J/mol K at room temperature.[27] Using this value gives $\Delta H° = -21$ kJ/mol, still in reasonable agreement with the ~-5 kJ/mol we calculated based on the 70 pN force quantum.

In the discussion above, we have used a rupture length of 1 Å, but the actual rupture length depends on the precise shape of the interaction potential along the trajectory that the two functional groups follow as they are pulled apart. If the TMPD and TCNQ groups in **I** and **II** are complexed in a face-to-face configuration, then a separation path perpendicular to the molecular planes, Scheme 3a, might yield a steeper potential and a larger rupture force than a path in which the functional groups slide out of contact, Schemes 3b and 3c. Under a tensile load, the molecules will follow a separation path that yields the smallest accessible potential gradient and thus the smallest rupture force. We conjecture that the molecules slide out of contact (Scheme 3b or 3c); this motion appears to be favored by the location of the alkane tethers and by the arrangement of the molecules between the probe and the substrate. Consequently, it is possible that the rupture length may be greater than 1 Å, which would increase the calculated bond energy. However, because the exact rupture length is not known, our bond energy estimate from the rupture force quantum can only be qualitatively compared with thermodynamic data. The value of 4−5 kJ/mol appears to be the right order of magnitude.

Another important consideration is that upon rupture of the CT complexes, it is possible that the redox active groups separate as molecular ions instead of neutral species. TMPD−TCNQ CT complexes can form from either the neutral molecules[28] or their ionic counterparts.[29] The electronic absorption spectrum in Figure 2A indicates that in the absence of any added electrolyte $CHCl_3$ solutions of **Ia** and **II** do contain a small concentration of the solvated molecular ions at equilibrium. The

(24) Hanson, A. W. *Acta Crystallogr.* **1965**, *19*, 610.
(25) (a) Ben-Tal, N.; Sitkoff, D.; Topol, I. A.; Yang, A.-S.; Burt, S. K.; Honig, B. *J. Phys. Chem. B* **1997**, *101*, 450. (b) Dixon, D. A.; Dobbs, K. D.; Valentini, J. J. *J. Phys. Chem.* **1994**, *98*, 13435.
(26) The force quanta determined from histograms recorded at different load rates were within the quoted experimental error.
(27) Rainville, D. P.; Zingaro, R. A.; Ferraris, J. P. *Can. J. Chem.* **1980**, *58*, 1133.
(28) Somoano, R.; Hadek, V.; Yen, S. P. S.; Rembaum, A.; Deck, R. *J. Chem. Phys.* **1975**, *62*, 1061.
(29) Michaelis, L.; Granick, S. *J. Am. Chem. Soc.* **1943**, *65*, 1747.

large excess of neutral molecules over molecular ions reflects the relative stability of the two species in $CHCl_3$. From a thermodynamic standpoint, the neutral species are heavily favored. Thus, we expect ionic separation to play a minor role in the rupture of the CT complexes in $CHCl_3$. If molecules **I** and **II** do separate as ions, then the $\Delta H°$ and $\Delta G°$ of complexation we considered above are not appropriate because they refer to the stability of the complex with respect to neutral donor and acceptor species. Instead we would need to compare our estimated bond energy with $\Delta H°$ for complex formation from the solvated donor and acceptor ions.

Modeling of Microcontact Pull-Off Forces. Another approach to verifying the interpretation of our measurements is to check whether the measured pull-off forces agree with the predictions of contact mechanics models. Previously, we reported a procedure for simulating the effect of specific interactions between the probe and the substrate in AFM pull-off force experiments.[9] Briefly, this procedure is based on the contact mechanics model of Johnson, Kendall, and Roberts[10] for a sphere of radius R interacting with a flat surface. The working equation of the model is

$$F_{\text{Pull-Off}} = \sqrt{\gamma_{\text{Solvent}}A - \gamma_{\text{Probe-Substrate}}n_{\text{Bonds}}\sigma}\sqrt{\frac{3Ka}{2}} \quad (6)$$

where γ_{Solvent} is the sum of the probe−solvent and substrate−solvent interfacial energies, $\gamma_{\text{Probe-Substrate}}$ is the probe−substrate interfacial energy, A is the contact area, a is the circular radius of the contact area at rupture, σ is the area per bond, and K is the elastic modulus of the probe−substrate contact. The parameter n_{Bonds} describes the actual number of bonds formed and is a binomial random variable with parameters $n_{\text{Max-bonds}}$, the maximum number of bonds possible within the contact area, and p, the probability of bond formation.[9]

Equation 6 returns a single pull-off force for given values of these variables. Real measurements give rise to a distribution of pull-off forces, as shown in Figures 4, 6, and 7. We have concluded that the distribution in forces is mainly attributable to contact area variations in successive contacts and to the bond formation probability, p. Thus, to introduce "white noise" into the output of eq 6, we input a Gaussian distribution of contact areas A in repetitive calculations of $F_{\text{Pull-Off}}$. If $p < 1$, there will be additional broadening.

The data in Figure 3 support our assumption that there are contact area variations in the pull-off experiments. Figure 3 shows that the force associated with consecutive pull-offs varies nonmonotonically. The nonmonotonic behavior suggests that the variation is not due to monolayer degradation. Instead, a probable cause of the variation in the force during consecutive measurements is the slow drift of the probe across the polycrystalline Au surface, resulting in gradual changes in the contact area. We can estimate the drift rate if we assume that the two minima observed in the average force (around the 90th and 260th force curves) correspond to the probe being on top of two adjacent Au grains 50 nm in diameter. The time elapsed between the minima is approximately 150 s which gives a drift rate of about 0.3 nm/s, a reasonable number.

The solvent interfacial energy terms needed for eq 6 can be estimated from pull-off measurements using eq 1. Measurements utilizing several probes with SAMs of **I** on both the probe and the substrate gave $\gamma_{\mathbf{I}-CHCl_3} = 0.13$ mJ/m^2. Equivalently,

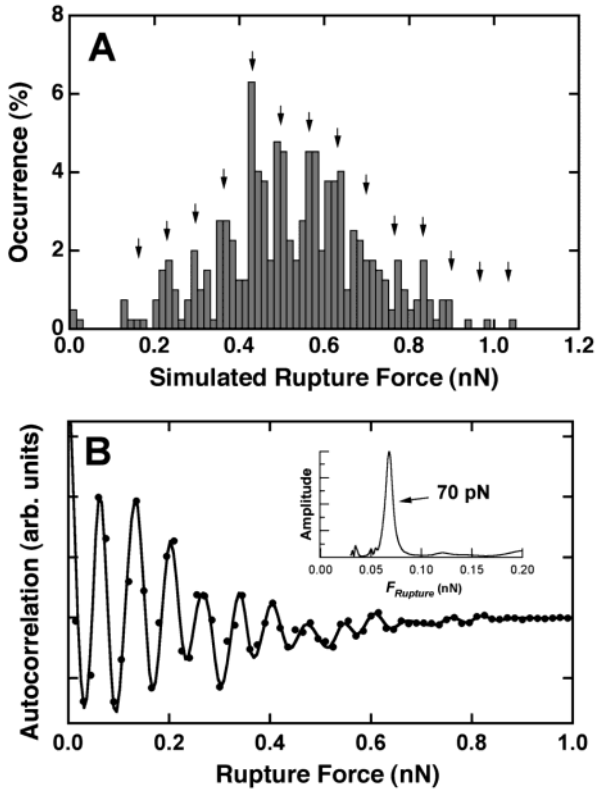

Figure 8. (A) Histogram of simulated pull-off forces. The individual peaks correspond to the rupture of integer numbers of TMPD−TCNQ CT complexes. The histogram was simulated using the following inputs to eq 6: $\gamma_{\text{Probe-Substrate}} = -2.0$ mJ/m^2, $\gamma_{\text{Solvent}} = 0.23$ mJ/m^2, $A = 4.9 \pm 2.3$ nm^2, $p = 0.9$, $\sigma = 0.7$ nm^2/molecule, and $K = 15$ GPa. The values of p, K, and the standard deviation for A were adjusted to match the histogram in Figure 4A. (B) The sinusoidal autocorrelation function of the histogram in (A) emphasizes the periodicity of peaks. The inset shows the Fourier transform of the autocorrelation.

measurements using SAMs of **II** gave $\gamma_{\mathbf{II}-CHCl_3} = 0.10$ mJ/m^2, yielding $\gamma_{\text{Solvent}} = 0.23$ mJ/m^2. Therefore, using eqs 1 and 2, we calculate that $\gamma_{\mathbf{I-II}}$ is -2.0 mJ/m^2.[30] We note that in order to detect single bond forces in pull-off experiments, $\gamma_{\text{Probe-Substrate}} < 0$ and $|\gamma_{\text{Probe-Substrate}}| > \gamma_{\text{Solvent}}$;[9] the interfacial energies important to this study meet these requirements. Analogous to our previous report,[14] the surface coverages of **I** and **II** were determined using cyclic voltammetry and are ~0.7 nm^2/molecule.

Our goal was to determine if pull-off force histograms generated by eq 6 reproduced key features of the experimental histogram in Figure 4A. Input parameters we considered fixed were the interfacial energies, $\gamma_{\text{Probe-Substrate}}$ and γ_{Solvent}, and the mean contact area A.[31] Adjustable parameters were the standard deviation of randomly generated contact area values around the mean, the probability of formation for each bond within the contact area, p, and the elastic modulus of the probe-substrate contact, K. Figure 8A shows a histogram of 400 calculated pull-off forces using $A = 4.9 \pm 2.3$ nm^2, $p = 0.9$, and $K = 15$ GPa as inputs.[32] The average contact area corresponds to $n_{\text{Max-bonds}} = 7$. Values for the other input parameters are listed in the figure caption. The histogram contains clearly distinguishable peaks

(30) The average rupture force from several AFM measurements involving SAMs of **I** and **II** was 0.42 nN. The average radius of curvature was 40 nm, which gives $W_{\text{Ad}} = 2.23$ mJ/m^2. With $\gamma_{\text{Solvent}} = 0.23$ mJ/m^2 we compute $\gamma_{\text{Probe-Substrate}} = -2.0$ mJ/m^2.

(31) The mean contact area A was determined from the average number of bonds being ruptured (seven bonds) and the area per bond (0.7 nm^2 per bond).

with an average periodicity of 70 pN, as emphasized by the sinusoidal autocorrelation function and the Fourier transform shown in Figure 8B. The mean force ($F^{Avg}_{Pull-Off} = 0.52$nN) is also comparable to the mean force in Figure 4A ($F^{Avg}_{Pull-Off} = 0.47$nN). Thus, using measured values for the interfacial energies, the average rupture force, and the surface coverage, and reasonable values for the three adjustable parameters as model inputs, we have obtained good correspondence with the experimental histogram. We note that we have shown that periodicity in the calculated histograms is not a forgone conclusion of the model.[9] Only when p is large and $|\gamma_{Probe-Substrate}| > \gamma_{Solvent}$ can single bond forces be detected. Thus, the correspondence we observe in Figure 8 supports our conclusion that the 70 pN periodicity observed in the histogram in Figure 4A is due to the rupture of an integer number of [TMPD−TCNQ] CT complexes.

In conclusion, we have shown for the first time that it is possible to detect single bond rupture forces in microcontact pull-off experiments involving SAM-modified AFM probes and substrates. We have focused specifically on detection of binding forces for discrete charge-transfer complexes formed at the interface between proximal SAMs bearing electron donors and acceptors. Histograms of hundreds of consecutive pull-offs reveal both a mean pull-off force and a 70 ± 15 pN force quantum that compare favorably with a contact mechanics model incorporating the effects of discrete chemical bonds, solvent surface tensions, and random contact area variations in consecutive pull-offs. The 70 pN force quantum also yields an estimate for the single bond energy of ∼4−5 kJ/mol, which is in reasonable agreement with available thermodynamic data. Key factors enabling the detection of single bond rupture forces are the strong, facile, and reversible nature of the CT bond and the relatively low interfacial energies between the SAMs and the solvent. Because SAMs can be prepared with a wide range of exposed functional groups, pull-off measurements between SAM-coated tips and substrates may provide a general strategy for directly measuring binding forces associated with a variety of simple, discrete chemical bonds, e.g., single hydrogen bonds or metal−ligand coordination interactions.

(32) In previous AFM studies, the value most commonly used for K is the value for an Au−Au contact (64 GPa, see for example refs 8g and 8k). As the measured rupture force gets smaller, however, the size of the contact area approaches molecular scale dimensions and K approaches the value for the SAM, ∼1 GPa.

Acknowledgment. H.S. and C.D.F. acknowledge the Center for Interfacial Engineering (CIE) at the University of Minnesota for financial support of this work.

JA028089R